arXiv:1001.3866v1 [cond-mat.str-el] 21 Jan 2010

A universal definition of the Kondo energy from the orthogonality catastrophe

Gerd Bergmann
Department of Physics
University of Southern California
Los Angeles, California 90089-0484
e-mail: bergmann@usc.edu

January 22, 2010

Abstract

The definitions of the Kondo energy in the numerical renormalization group (NRG) and the Friedel artificially inserted resonance (FAIR) theory fail sadly for small samples where their predicted Kondo energy increases, while in reality the Kondo effect disappears. Therefore a different, universal definition of the Kondo energy is proposed, which uses the evasion of the orthogonality catastrophe by the Kondo impurity. A magnetic impurity which has a pure diagonal interaction $2Js_zS_z$ with the conduction electrons polarizes all of the spin-up and down electrons and reduces the scalar product between corresponding spin-up and down states. The multi-electron scalar product (MESP) between all occupied spin-up and spin-down states approaches zero exponentially with the number N of Wilson states (this is the so-called orthogonality catastrophe). In contrast in the Kondo ground state the corresponding conduction electrons of opposite spin are pairwise aligned within the Kondo energy. In the present paper the MESP is investigated for the FAIR solution of the Friedel-Anderson impurity. The MESP is numerically determined for the (enforced) magnetic and the singlet states as a function of the number N of Wilson states. The magnetic states show an exponentially decreasing MESP as a function of N. Surprisingly it is not the number of states which causes this decrease. It is instead the smallest energy separation from the Fermi energy that determines the reduction of the MESP. In the singlet state the ground state requires a finite MESP to optimize its energy. As a consequence there is no orthogonality catastrophe. The MESP approaches a saturation value as function of N. Within the energy range of the Kondo energy the scalar product between corresponding (single electron) spin-up and spin-down states is very close to 1.000 and falls off beyond the Kondo energy. The energy which separates the two regions is well suited as a universal definition of the Kondo energy.

PACS: 75.20.Hr, 71.23.An, 71.27.+a

1 Introduction

There are many definitions of the Kondo temperature in the theoretical solid state literature. The first one was derived from the divergence of the perturbation calculation. It yielded essentially

$$k_B T_K \approx D \exp\left[-\frac{1}{2\rho_0 J}\right]$$

where ρ_0 is the density of states, J is the exchange constant in the interaction $2J\mathbf{s}\cdot\mathbf{S}$, and D is half the band width. The exact definition depends on the extent to which different families of diagrams are included in the calculation.

In numerical calculations one generally uses a second generation definition for the Kondo energy. For example the numerical renormalization group (**NRG**) theory defines the Kondo energy ε_K as a quarter of the inverse susceptibility $\chi(T=0)$ of the spin 1/2 impurity at zero temperature.

$$\varepsilon_K = \frac{1}{4\chi(T=0)}$$

In the FAIR theory (Friedel artificially inserted resonance) our group uses the singlet-triplet excitation energy. There are two such energies, E_{st} and E^*_{st}. While the first one is just the excitation energy using the optimal bases in the singlet state the energy E^*_{st} is obtained by optimizing the FAIR solution also in the triplet state and using the lowest possible triplet energy as the excited state. Generally E^*_{st} is smaller than E_{st} by a factor not very different from four. On the other hand the energy E_{st} is almost equal to χ^{-1}. Therefore the NRG and the FAIR definitions are very close. (Here a 30% deviation is considered as close).

I consider these definitions of the Kondo energy as second generation because they cannot be universally applied. One important example where they fail is small samples. It is well known that the Kondo effect disappears when the sample size becomes too small (although there were many controversies about the critical size to show the Kondo effect). The Kondo effect requires a sufficient number of states in the energy regime $-\varepsilon_K < \varepsilon < \varepsilon_K$ where the energy ε is measured from the Fermi level. Although the Kondo effect disappears with decreasing sample size, neither the susceptibility nor the singlet-triplet excitation energy disappear. On the contrary both increase with decreasing sample size. They are obviously not a first class measure for the Kondo energy. Actually our group ran into this problem while investigating small samples. Therefore we had to find a more appropriate definition of the Kondo energy. I think we have found a unique and universal criterion in the way the Kondo effect circumvents the orthogonality catastrophe. This paper is organized as follows: In chapter II the orthogonality catastrophe of the Friedel-Anderson (**FA**) impurity in the magnetic state is discussed within the frame work of the FAIR theory. In chapter III numerical results for the multi-electron scalar product are presented in the enforced magnetic and the singlet state. Its dependence on the number of states, the smallest energies, and other parameters is investigated. It turns out that in the Kondo ground state the (single) electron states for spin up and down are aligned close to the Fermi level within the Kondo energy. In chapter IV this alignment is investigated quantitatively and a procedure is developed to

extract the Kondo energy ε_K from this alignment.

2 Orthogonality catastrophe

The orthogonality (or infrared) catastrophe was introduced and discussed already 40 years ago [1], [2], [3], [4]. An example is a magnetic impurity in a metal host which interacts with the conduction electron in the form $H' = 2J(\mathbf{r})\,\mathbf{s}\cdot\mathbf{S}$. The effect of the z-component $2J(\mathbf{r})\,s_zS_z$ is the following. Let the spin direction of the impurity point upwards. Then the wave function of the conduction electrons is pulled towards or pushed away from the impurity, depending on the electron spin. As a consequence the scalar product of corresponding s-electron states with opposite spin is slightly less than 1.

If we denote the resulting (modified) bases for spin up and down as $\left\{c^\dagger_{\nu+}\right\}$ and $\left\{c^\dagger_{\nu-}\right\}$ with N states in each basis ($1 \le \nu < N$), and if half the spin-up and down sub-bands are occupied then the value of the multi-electron scalar product (**MESP**) between all occupied s-states with spin up and those with spin down is defined by the determinant

$$M^{(N/2)} = \begin{vmatrix} \left\langle c^\dagger_{1,+}|c^\dagger_{1,-}\right\rangle & \left\langle c^\dagger_{1,+}|c^\dagger_{N/2,-}\right\rangle \\ \left\langle c^\dagger_{N/2,+}|c^\dagger_{1,-}\right\rangle & \left\langle c^\dagger_{N/2,+}|c^\dagger_{N/2-}\right\rangle \end{vmatrix}$$

The common argument is that the multi-electron scalar product between all occupied s-states with spin up and those with spin down approaches zero when N, and therefore the number of occupied s-electron states, becomes very large. Now we add to this system of spin-up impurity plus polarized conduction electrons the time reversed system where all spin directions are reversed. Then the matrix element for a transition between the two states by spin-flip processes of the form $J(\mathbf{r})\,[s^+S^- + s^-S^+]$ vanishes. Therefore the system cannot decrease its energy by spin-flip processes. However, at small energy states the gain in spin-flip energy is larger than the gain in spin polarization. Therefore the non-diagonal part of the $\mathbf{s}\cdot\mathbf{S}$ interaction tries to prevent the orthogonality catastrophe. This can be well traced in the FAIR treatment of the Kondo impurity.

In the following the Friedel-Anderson (FA) impurity will be discussed where this process is less obvious. The Hamiltonian for the FA-impurity is given by

$$H_{FA} = \sum_\sigma \left\{ \sum_{\nu=1}^{N} \varepsilon_\nu c^\dagger_{\nu,\sigma}c_{\nu,\sigma} + E_d d^\dagger_\sigma d_\sigma + \sum_{\nu=1}^{N} V_{sd}(\nu)[d^\dagger_\sigma c_{\nu,\sigma} + c^\dagger_{\nu,\sigma}d_\sigma] \right\} + U n_{d\uparrow}n_{d\downarrow} \qquad (1)$$

In the following I assume that the reader is familiar with the FAIR method which our group developed during the past few years [5], [6], [7]. A short review is posted at the ArXiv [8].

Krishna-murthy, Wilkins, and Wilson [9] clarified the role of the local magnetic moment in the FA-impurity. They performed a numerical renormalization a la Wilson [10] for the

FA-Hamiltonian. They demonstrated that for sufficiently large Coulomb repulsion (when $U >> \Gamma = \pi\rho\left|V_{sd}\right|^2$) the flow of their Hamiltonian H_N passed close to the fixed point for a local moment. This means that under these conditions the impurity first assumed a magnetic moment when the temperature is lowered. After passing the fixed point for the local moment the renormalization flow (corresponding to a reduction of temperature) approaches the Kondo ground state.

In the following I will discuss the two different solutions of the FA-Hamiltonian: the magnetic state and the singlet state. (The magnetic state can be enforced by a small magnetic field). This state will be called the **enforced magnetic state**. This avoids the finite temperature treatment. In FAIR the magnetic solution Ψ_{MS} has the form

$$\Psi_{MS} = \left[Aa^{\dagger}_{0-\downarrow}a^{\dagger}_{0+\uparrow} + Bd^{\dagger}_{\downarrow}a^{\dagger}_{0+\uparrow} + Ca^{\dagger}_{0-\downarrow}d^{\dagger}_{\uparrow} + Dd^{\dagger}_{\downarrow}d^{\dagger}_{\uparrow}\right]\prod_{i=1}^{n-1}a^{\dagger}_{i-\downarrow}\prod_{i=1}^{n-1}a^{\dagger}_{i+\uparrow}\Phi_0 \tag{2}$$

The states states $a^{\dagger}_{0+}$ and $a^{\dagger}_{0-}$ are FAIR states. The coefficients A, B, C, D and the compositions of the FAIR states are optimized to minimize the energy expectation value of the FA Hamiltonian. Due to the condition $\left\langle a^{\dagger}_{i\tau}\Phi_0\left|H_0\right|a^{\dagger}_{j\tau}\Phi_0\right\rangle = 0$ the FAIR states determine the other states $a^{\dagger}_{i\tau}$ of the basis $\left\{a^{\dagger}_{i\tau}\right\}$ uniquely (where $i, j > 0$, H_0 is the free electron Hamiltonian and $\tau = +, -$).

The singlet state is a symmetric superposition of a magnetic state and its time- (or spin-) reversed state. (The FAIR states $a^{\dagger}_{0+}$ and $a^{\dagger}_{0-}$ and the coefficients A, B, C, D are independently optimized for the magnetic and singlet states).

For the FAIR solution the MESP between the occupied spin up and spin down sub-bands is essentially given by

$$M^{(N/2)}_{+-} = \left\langle \prod_{i=0}^{N/2-1}a^{\dagger}_{i+}\Phi_0\right| \prod_{j=0}^{N/2-1}a^{\dagger}_{j-}\Phi_0\Bigg\rangle \tag{3}$$

3 Numerical Calculation of the Multi-Electron Scalar Product

3.1 The enforced magnetic state

For most of the numerical calculations Wilson states are used (see appendix). In the calculation the following parameters are used: $\left|V_{sd}\right|^2 = 0.1$, $U = 1, E_d = -0.5$. The magnetic solution is optimized for different numbers of Wilson states with $N = 20, 30, 40, 50, 60$. Table I shows $M^{(N/2)}_{MS}$ of the magnetic solution for the different sizes N of the bases. The third column gives the scalar product of the two FAIR states, $\langle a_{0+}\Phi_0|a_{0-}\Phi_0\rangle_{MS}$, the fourth column the ground-state energy, and the fifth column gives the magnetic moment. (Φ_0 is the vacuum state). As one can see the scalar product $\langle a_{0+}\Phi_0|a_{0-}\Phi_0\rangle_{MS}$, the ground-state energy

(in the enforced magnetic state), and the moment have reached their final values already for $N = 30$. However, the multi-scalar product decreases with increasing N.

N	$M_{MS}^{(N/2)}$	$\langle a_{0+}\|a_{0-}\rangle_{MS}$	$E_{0,MS}$	μ	$\langle a_{N/2}\|a_{N/2}\rangle_{MS}$
10	0.878	0.823	-0.607799	0.514	.92
20	0.396	0.501	-0.627446	0.687	.64
30	0.190	0.4852	-0.62810	0.690	.55
40	0.0917	0.4845	-0.62812	0.690	.52
50	0.0443	0.4845	-0.62812	0.690	.50
60	0.0216	0.484	-0.62812	0.690	.49
2*20	0.394	0.526	-0.629323	0.66	.64
2*30	0.198	0.514	-0.629779	0.67	.57

Table I: The multi-electron scalar product (MESP) and other parameters for the Friedel-Anderson impurity in the enforced magnetic state. The different columns give the number of Wilson states, the MESP, the (single electron) scalar product $\langle a_{0+}\Phi_0|a_{0-}\Phi_0\rangle_{MS}$ between the two FAIR states, the ground-state energy, and the magnetic moment. The 6th column is explained in the text. The parameters used in the calculation are $|V_{sd}|^2 = 0.1$, $U = 1, E_d = -0.5$.

In Fig.1 the logarithm of the multi-electron scalar product $\ln\left(M_{MS}^{(N/2)}\right)$ is plotted versus the number of Wilson states N. It follows a straight line which corresponds to the relation

$$M_{MS}^{(N/2)} = 1.7e^{-0.073*N} = 1.7 * 0.93^{-N}$$

Obviously, the multi-scalar product decreases exponentially with increasing N.

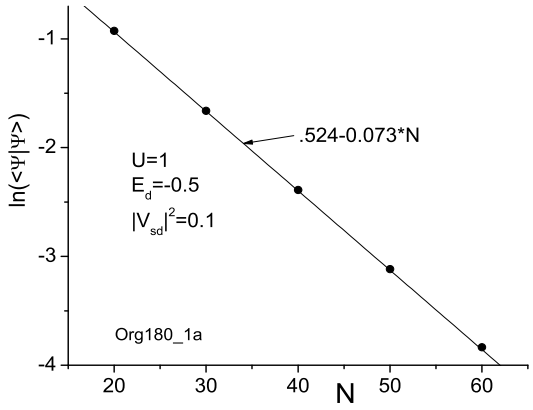

Fig.1: The logarithm of the multi-electron scalar product MESP $\left\langle \prod_{i=0}^{n-1} a_{i+}^{\dagger}\Phi_0 | \prod_{i=0}^{n-1} a_{i-}^{\dagger}\Phi_0 \right\rangle$ is plotted versus the number of Wilson states N with $n = N/2$ for the magnetic state.

In the next step I check whether it is just the number of states N which reduces $M_{MS}^{(N/2)}$. For this purpose the N energy cells for $N = 20$ and 30 are sub-divided into two. This is achieved by using $\Lambda = \sqrt{2}$. This doubles the number of Wilson states but adds only one state (for positive and negative energy) closer to the Fermi level. The results of this calculation are collected at $N = 2 * 20$ and $2 * 30$. It turns out that the doubling has essentially only a minor effect on $M_{MS}^{(N/2)}$. This is on a first sight rather surprising since it was believed that the increase of the number of states causes the orthogonality catastrophe of the MESP.

To further confirm this observation I take the energy frame with $N = 20$ and subdivide the energy range $(-1 : -1/4)$ into cells with a width of $1/8$, replacing two Wilson states by six new states. (The same is done for the positive range). This changes $M_{MS}^{N/2}$ from 0.396 to 0.405. Splitting the same energy range into 14 cells with a width of $1/32$ yields the MESP $M_{MS}^{N/2} = 0.411$. This shows that increasing N by subdividing an energy range does not contribute to an orthogonality catastrophe (as long as the energy range does not border the Fermi level at the energy 0).

On the other hand, the smallest (absolute) energies have a great impact on the MESP. To investigate this question further I take the energies for $N = 20$ and shift the two states which are closest to the Fermi level towards the latter. The four energy cells which are closest to the Fermi level are $\mathfrak{C}_9 = (-2^{-8} : -2^{-9})$, $\mathfrak{C}_{10} = (-2^{-9} : 0)$, $\mathfrak{C}_{11} = (0 : 2^{-9})$, $\mathfrak{C}_{12} = (2^{-9} : 2^{-8})$. I replace $\pm 2^{-9}$ by $\pm 2^{-19}$. Then the (average) energies of the corresponding states are $\varepsilon_9 = -\frac{2049}{1048\,576} \approx -1.954\,1 \times 10^{-3}$, $\varepsilon_{10} = -2^{-20}$, $\varepsilon_{11} = 2^{-20}$ and $\varepsilon_{12} = 1.954\,1 \times 10^{-3}$. Of course this reduces the s-d interaction strength $V_{sd}(\nu)$ for $\nu = 10, 11$ from $[2^{-9}/2]^{1/2} = 2^{-5}$ to $[2^{-19}/2]^{1/2} = 2^{-10}$.

After optimizing the $\{a_{i+}\}$ and $\{a_{i-}\}$ bases and the coefficients A, B, C, D the resulting MESP is reduced to $M_{MS}^{10} = 0.0208$. The number of states is still $N = 20$. The shifting of the smallest energies from $\pm 2^{-10}$ to $\pm 2^{-20}$ changes the value of the MESP from 0.396 to 0.0208. This shows that the value of the MESP is determined by the occupied state closest to the Fermi level. The total number of states is only important when it determines the energy of this state.

3.2 The singlet state

In the next step I calculate the MESP for the singlet ground state. The same parameters $|V_{sd}|^2 = 0.1$, $U = 1, E_d = -0.5$ are used as in table I and Fig.1. The FAIR solution for the singlet state is obtained by reversing all spins in Ψ_{MS} and combining the two states.

$$\Psi_{SS} = \Psi_{MS}(\uparrow\downarrow) + \Psi_{MS}(\downarrow\uparrow)$$

$$= \left[A a^\dagger_{0-\downarrow} a^\dagger_{0+\uparrow} + B d^\dagger_\downarrow a^\dagger_{0+\uparrow} + C a^\dagger_{0-\downarrow} d^\dagger_\uparrow + D d^\dagger_\downarrow d^\dagger_\uparrow \right] \prod_{i=1}^{n-1} a^\dagger_{i-\downarrow} \prod_{i=1}^{n-1} a^\dagger_{i+\uparrow} \Phi_0 \tag{4}$$

$$+ \left[A' a^\dagger_{0-\uparrow} a^\dagger_{0+\downarrow} + B' d^\dagger_\uparrow a^\dagger_{0+\downarrow} + C' a^\dagger_{0-\uparrow} d^\dagger_\downarrow + D' d^\dagger_\uparrow d^\dagger_\downarrow \right] \prod_{i=1}^{n-1} a^\dagger_{i-\uparrow} \prod_{i=1}^{n-1} a^\dagger_{i+\downarrow} \Phi_0$$

The coefficients $A, B, C, D, A', B', C', D'$ and the compositions of the FAIR states $a^\dagger_{0+}$ and $a^\dagger_{0-}$ are again optimized to minimize the energy expectation value of the FA Hamiltonian. In table II the corresponding data are collected. Again the first four columns give the same data as in table I, i.e. the number of Wilson states, the MESP, the (single electron) scalar product between the two FAIR states $a^\dagger_{0+}$ and $a^\dagger_{0-}$ and the ground-state energy. The 5th column gives the Kondo energy defined as the difference between the relaxed triplet energy and the singlet ground-state energy. The relaxed triplet energy is obtained by setting the primed coefficients X' in equ. (4) opposite equal to the coefficient without prime X and minimizing the energy.

Dependence on the number of states N

N	$M_{SS}^{(N/2)}$	$\langle a_{0+} \vert a_{0-} \rangle_{SS}$	$E_{0,SS}$	ΔE	$>.999$
10	0.749	0.645	-0.62272	14.8×10^{-3}	
20	0.742	0.6448	-0.637535	10.1×10^{-3}	9-10
30	0.742	0.6448	-0.637965	9.87×10^{-3}	9-21
40	0.742	0.6448	-0.63798	9.86×10^{-3}	9-31
50	0.742	0.6448	-0.63798	9.86×10^{-3}	9-41
60	0.742	0.6448	-0.637973	9.85×10^{-3}	9-51
2*20	0.751	0.657	-0.639684	10.4×10^{-3}	17-23
2*30	0.751	0.657	-0.639993	10.2×10^{-3}	18-43

Table II: The multi-electron scalar product (MESP) and other parameters for the Friedel-Anderson impurity in the singlet state. The different columns give the number of Wilson states N, the MESP, the (single electron) scalar product $\langle a_{0+}\Phi_0 \vert a_{0-}\Phi_0 \rangle_{MS}$ between the two FAIR states, the ground-state energy, and the Kondo energy. The 6th column is explained in the text. The parameters used in the calculation are $\vert V_{sd} \vert^2 = 0.1$, $U = 1$, $E_d = -0.5$.

For the last column I calculated the scalar product $\left\langle a^\dagger_{+,i}\Phi_0 \vert a^\dagger_{-,j}\Phi_0 \right\rangle$ for all pairs of (i, j) which form a $N \times N$-matrix. It turns out that the diagonal elements $\left\langle a^\dagger_{+,i}\Phi_0 \vert a^\dagger_{-,i}\Phi_0 \right\rangle$ close to the Fermi energy approach the value one. For example if the sixth column shows for $N = 30$ the value "$9 - 21$" then the values of the (single particle) scalar products $\left\langle a^\dagger_{+,i}\Phi_0 \vert a^\dagger_{-,i}\Phi_0 \right\rangle$ lie between 0.999 and 1.000 for $9 \leq i \leq 21$. Obviously the states $a^\dagger_{+,i}$ and $a^\dagger_{-,i}$ are almost identical in this interval. This is very different for the enforced magnetic state. There, in

table I the 6th column shows the value of the diagonal scalar product for $i = N/2$ and the larger one of its two neighbors $\left\langle a^\dagger_{+,N/2}\Phi_0 | a^\dagger_{-,N/2\pm1}\Phi_0 \right\rangle$.

Dependence on the interaction $|V_{sd}|^2$

The MESP in the singlet state depends on the strength of the s-d interaction. Keeping the number of Wilson states constant $N = 40$, the MESP is numerically determined and collected in table III.

$\|\mathbf{V}_{sd}\|^2$	$M_{SS}^{(N/2)}$	$\left\langle a^\dagger_{0+} \| a^\dagger_{0-} \right\rangle_{SS}$	$E_{0,SS}$	ΔE	$>.999$
0.10	0.742	0.645	-0.637977	9.86×10^{-3}	-
0.09	0.708	0.604	-0.621392	8.13×10^{-3}	10-30
0.08	0.665	0.553	-0.605078	6.14×10^{-3}	10-30
0.07	0.607	0.489	-0.589200	4.09×10^{-3}	11-29
0.06	0.527	0.406	-0.573975	2.22×10^{-3}	11-29
0.05	0.407	0.299	-0.559655	8.21×10^{-4}	12-28

Table III: The multi-electron scalar product (MESP) and other parameters for the Friedel-Anderson impurity in the singlet state. The columns give the s-d interaction $|V_{sd}|^2$, the MESP, the scalar product $\left\langle a^\dagger_{0+}\Phi_0 | a^\dagger_{0-}\phi_0 \right\rangle$, the ground-state energy, and Kondo energy ΔE. The 6th column is explained in the text. The parameters used in the calculation are $U = 1, E_d = -0.5$ and the number of Wilson states is $N = 40$.

In Fig.2 the logarithm of the Kondo energy is plotted versus the logarithm of the MESP. A linear dependence is obtained. The MESP shows a weak dependence on the Kondo energy with a power of about 1/4.

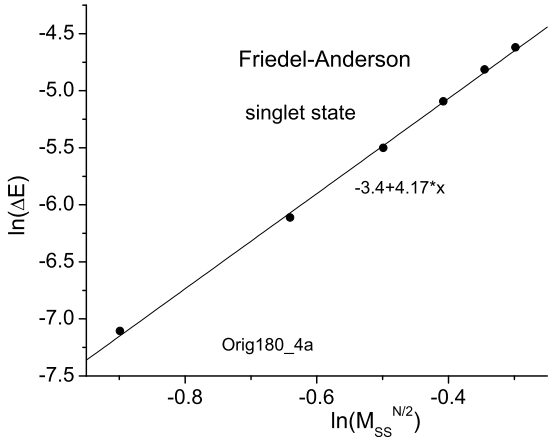

Fig.2: The log-log plot of the Kondo energy versus the MESP for the singlet state for different s-d interactions.

4 State alignment within the Kondo energy

4.1 Friedel-Anderson impurity

The states $a^\dagger_{+,i}$ are constructed from the basis $c^\dagger_\nu$ by extracting a FAIR state $a^\dagger_{+,0}$. Therefore the states $a^\dagger_{+,i}$ and $c^\dagger_\nu$ are pairwise quite similar except that there is one state missing in the basis $\{a_{+,i}\}$. The same applies to the states $a^\dagger_{-,i}$ and $c^\dagger_\nu$.

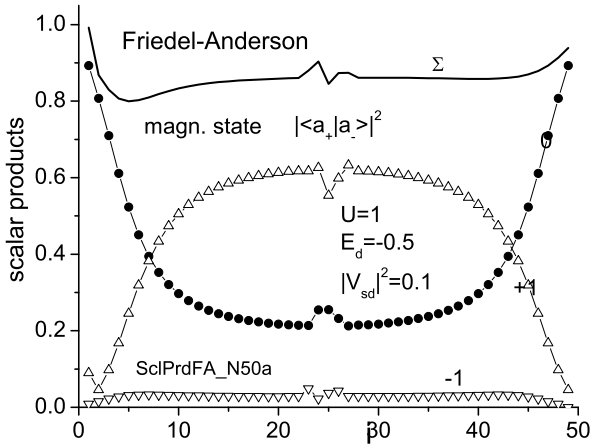

Fig.4: The square of the diagonal matrix-elements $\left|\left\langle a^\dagger_{+,i}\Phi_0|a^\dagger_{-,i}\Phi_0\right\rangle\right|^2$ as well as the next-to-diagonal matrix-elements $\left|\left\langle a^\dagger_{+,i}\Phi_0|a^\dagger_{-,i\pm1}\Phi_0\right\rangle\right|^2$ are plotted as a function of i for the enforced magnetic state.

As a consequence the two bases $\left\{a^\dagger_{+,i}\right\}$ and $\left\{a^\dagger_{-,i}\right\}$ are also quite similar. In Fig.4 the single-particle scalar products $\left|\left\langle a^\dagger_{+,i}\Phi_0|a^\dagger_{-,i}\Phi_0\right\rangle\right|^2$ for the enforced magnetic state are plotted as a function of i (full circles). In addition $\left|\left\langle a^\dagger_{+,i}\Phi_0|a^\dagger_{-,i\pm1}\Phi_0\right\rangle\right|^2$ are plotted as empty up and down triangles. The full curve (without symbols) gives the sum of the three contributions. One recognizes that an arbitrary state $a^\dagger_{+,i}$ (for $i > 0$) consists 80% out of the states $a^\dagger_{-,i}, a^\dagger_{-,i+1}$ and $a^\dagger_{-,i-1}$. On the other hand $a^\dagger_{+,i}$ and $a^\dagger_{-,i}$ overlap only 30% for small energies (in the center of the horizontal axis).

This is very different for the singlet state. In Fig.5 the single-electron scalar products $\left|\left\langle a^\dagger_{+,i}\Phi_0|a^\dagger_{-,i}\Phi_0\right\rangle\right|^2$ as well as $\left|\left\langle a^\dagger_{+,i}\Phi_0|a^\dagger_{-,i\pm1}\Phi_0\right\rangle\right|^2$ are plotted as a function of i for the singlet state. One recognizes that over a large energy range the states $a^\dagger_{+,i}$ and $a^\dagger_{-,i}$ are 99% or more identical. Only for (absolute) large energies on the left and right side is the overlap reduced

to about 70%.

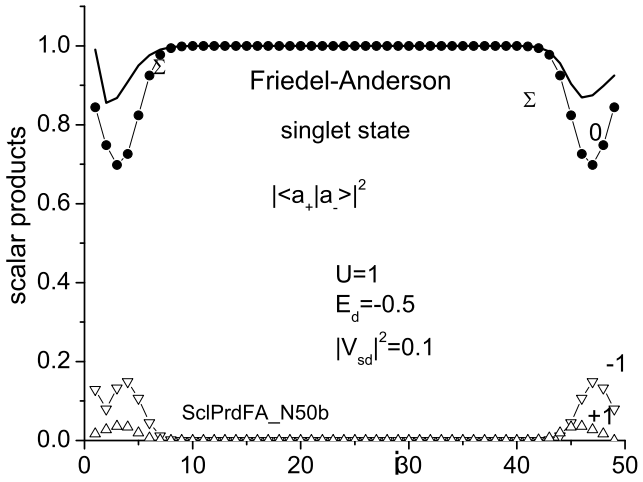

Fig.5: The square of the diagonal matrix-elements $\left|\left\langle a^\dagger_{+,i}\Phi_0|a^\dagger_{-,i}\Phi_0\right\rangle\right|^2$ as well as the next-to-diagonal matrix-elements $\left|\left\langle a^\dagger_{+,i}\Phi_0|a^\dagger_{-,i\pm1}\Phi_0\right\rangle\right|^2$ are plotted as a function of i for the singlet state.

The reason for this different behavior is rather transparent. The energy expectation value of the enforced magnetic state does not depend on the MESP. The s-d transitions happen only within the same spin orientation and therefore within the same basis. There is no advantage of having the states $a^\dagger_{+,i}$ and $a^\dagger_{-,i}$ aligned.

On the other hand in the singlet state one has transitions from

$$a^\dagger_{0-\downarrow}a^\dagger_{0+\uparrow}\prod_{i=1}^{n-1}a^\dagger_{i-\downarrow}\prod_{i=1}^{n-1}a^\dagger_{i+\uparrow}\Phi_0 <=> d^\dagger_\uparrow a^\dagger_{0+\downarrow}\prod_{i=1}^{n-1}a^\dagger_{i-\uparrow}\prod_{i=1}^{n-1}a^\dagger_{i+\downarrow}\Phi_0$$

Such a transition is proportional to the square of the MESP. To be able to harvest energy from these processes the states $a^\dagger_{i+}$ and $a^\dagger_{i-}$ are, for small energies, aligned with each other.

The next question investigated is how the alignment of the states $a^\dagger_{i+}$ and $a^\dagger_{i-}$ depends on the energy $E_{i,\pm}$ of the states $a^\dagger_{i+}$ and $a^\dagger_{i-}$. In Fig.6 the scalar product $\left\langle a^\dagger_{i+}\Phi_0|a^\dagger_{i-}\Phi_0\right\rangle$ is plotted as a function of $\log|E_{i,\pm}|$ for the parameters $|V_{sd}|^2 = 0.04$, $E_d = -0.5$ and $U = 1.0$. One recognizes that for positive and negative energies the scalar product at small energies is essentially equal to one. Then at larger energies the values of the scalar product decrease in first approximation linearly. The intersection of the two straight lines is at $\log|E_{i,\pm}| = -3.41$. The corresponding energy of 3.90×10^{-4} can be used as a new definition for the Kondo energy.

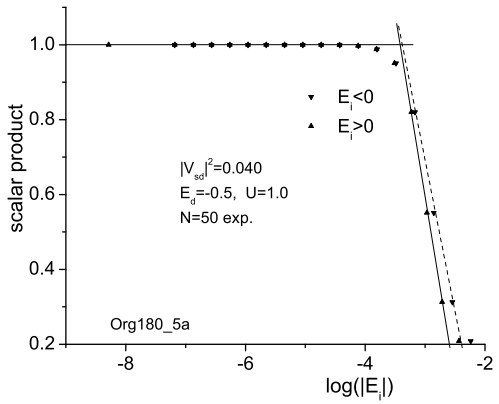

Fig.6: The scalar product $\left\langle a^\dagger_{+,i}\Phi_0|a^\dagger_{-,i}\Phi_0\right\rangle$ as a function of the logarithm of the absolute value of the energies $\log|E_{i,\pm}|$. The parameters are $|V_{sd}|^2 = 0.04$, $E_d = -0.5$ and $U = 1.0$ for the Friedel-Anderson impurity.

In Fig.7 a similar plot is shown for different values of $|V_{sd}|^2$. The smaller the value of $|V_{sd}|^2$ the smaller is the energy of the intersection. For the value of 0.02 the scalar product never reaches the value one. For this value the Kondo energy is less than 10^{-9}. For $N = 50$ the smallest energy of the states $c^\dagger_\nu$ (and correspondingly for $a^\dagger_{i,\pm}$) is $2^{-25} \approx 3 \times 10^{-8}$. This corresponds also to a $\Delta k = |k - k_F| \approx 3 \times 10^{-8}$ (k is the wave number is the corresponding state). Through the uncertainty principle (or through the quantization condition $\Delta k = \pi/R$) this corresponds to a finite sample radius of $R \approx 1. \times 10^8$ (see appendix).

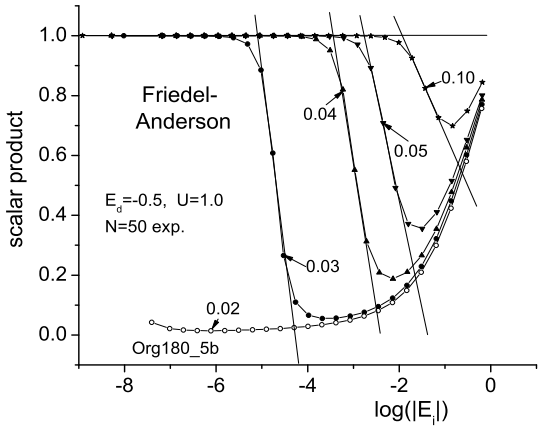

Fig.7: The scalar product $\left\langle a^\dagger_{+,i}\Phi_0|a^\dagger_{-,i}\Phi_0\right\rangle$ as a function of $\log|E_{i,+}|$ for the different s-d-coupling in the Friedel-Anderson impurity. The value of $|V_{sd}|^2$ is shown next to the curves. The d-state and Coulomb energies are $E_d = -0.5$ and $U = 1.0$.

In Fig.8 the different results are collected. Here the extrapolated logarithm of the energy $\log(\varepsilon_K)$ is used as abscissa. For each parameter set the logarithm of the unrelaxed singlet-triplet energy $\log(E_{st})$ (full circle), the relaxed singlet-triplet energy $\log(E^*_{st})$ (full triangle) and the susceptibility energy $\log(E_\chi)$ (stars) are plotted). Here E_χ is defined by the inverse susceptibility as $E_\chi = 1/(4\chi)$. (The latter has been recently calculated for the

FAIR approach [11].) Along the straight line abscissa and ordinate are equal. The different definitions for the Kondo energy yield rather similar results. The new definition yields slightly larger values than the susceptibility and the relaxed E^*_{st}, but smaller values than the unrelaxed one E_{st}.

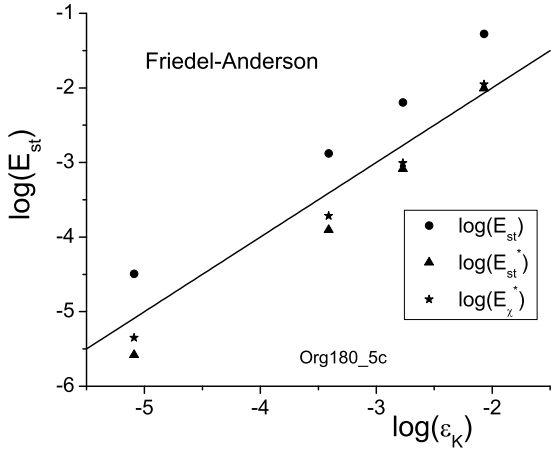

Fig.8: The logarithm of the unrelaxed energy E_{st} (full circle), relaxed E^*_{st} (triangle) and susceptibility energy E_χ as a function of the logarithm of the extrapolated energy ε_K. The straight line corresponds to $\log(E_{st}) = \log(\varepsilon_K)$.

4.2 Kondo impurity

The same calculations are performed for the Kondo impurity. In Fig.9 a similar plot is shown for different values of J. The smaller the value of J the smaller is the energy of the intersection.

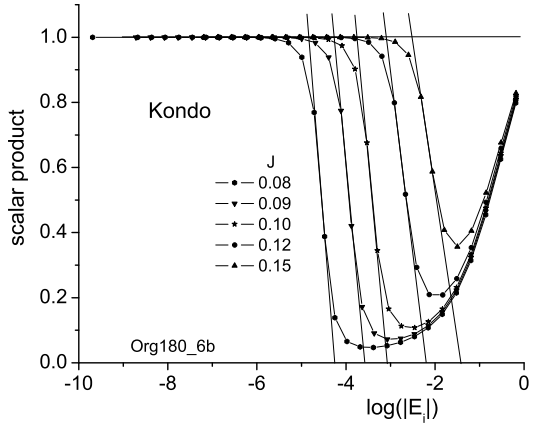

Fig.9: The scalar product $\left\langle a^\dagger_{+,i}\Phi_0 | a^\dagger_{-,i}\Phi_0 \right\rangle$ as a function of $\log|E_{i,+}|$ for the different s-d-coupling in the Kondo impurity. The values of J are shown next to the curves.

In Fig.10 the different results are collected. Again the extrapolated logarithm of the energy ε_K is used as abscissa. For each parameter set the logarithm of the unrelaxed singlet-triplet energy $\log(E_{st})$ (full circle), the relaxed singlet-triplet energy $\log(E^*_{st})$ (full triangle) and the susceptibility energy $\log(E_\chi)$ (stars) are plotted). Again the different values are essentially proportional to each other.

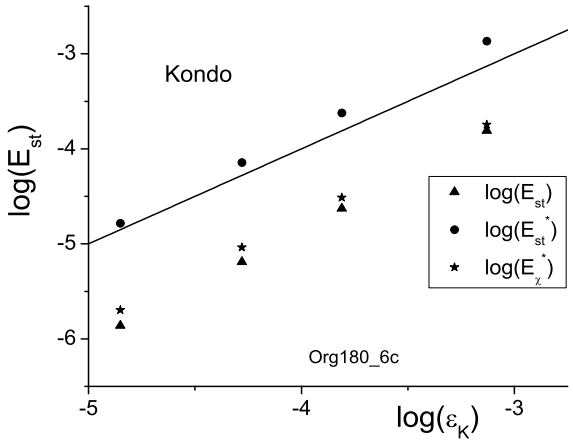

Fig.10: The logarithm of the unrelaxed energy E_{st} (full circle), relaxed E^*_{st} (triangle) and susceptibility energy E_χ as a function of the logarithm of the extrapolated energy ε_K.

5 Conclusion

The Kondo effect develops only in samples of sufficiently large size. This is (at least) known since Wilson's NRG paper. However, two of the measures for the Kondo energy, the suceptibility energy and the singlet-triplet excitation energy increase when the sample size is decreased. Both fail as a measure for the Kondo energy for small sample sizes. In the present paper the alignment of the electronic wave functions close to the Fermi energy is proposed as an alternative measure for the Kondo energy. This alignment is intimately connected to the Kondo ground state. In the Kondo ground state the alignment takes place to avoid the orthogonality catastrophe. The latter prevents any energy gain of the ground-state energy from spin-flip processes. Therefore the energy range in which spin-up and down electron states are aligned is also the energy range in which spin-flip processes contribute to the reduction of the ground-state energy. Since this energy range is exponentially small the Kondo energy is exponentially small.

A satisfactory definition of the Kondo energy that shows the disappearance of the Kondo effect is required to investigate the presence (or absence) of the Kondo effect in small samples, in particular in three dimensions. It was long believed that the critical size for the Kondo

effect in three dimensions is the Kondo radius $r_K = \hbar v_F/\varepsilon_K$. (In Wilson nomiclature $\hbar v_F$ is equal to one). The author [12] investigated the conditions for the development of a resonance in three dimensions. Only a perfect sphere with the impurity in the center requires such a large size as $\hbar v_F/\varepsilon_R$ (where ε_R is the energy width of the resonance). For less symmetric samples a much smaller size is sufficient. Presently our group is investigating this question for the Kondo resonance. The criterion developed here for the Kondo energy and the occurrence of the Kondo effect is essential for this investigation.

6 Appendix

A Kondo Effect in Small Samples

As mentioned above one can simulate a small sample by using a finite number of Wilson states. Wilson [10] in his Kondo paper considered an s-band ranging from -1 to 1 with a constant density of states. Then Wilson replaced the energy continuum of s-states by a discrete set of cells. First the negative energy band is subdivided on a logarithmic scale. The discrete energy values are $-1, -1/\Lambda, -1/\Lambda^2, -\Lambda^{-\nu}, .. - \Lambda^{-(N/2-1)}, 0$. (More often than not the value chosen for Λ is 2). These discrete points $\xi_\nu = -\Lambda^{-\nu}$ are used to define a sequence of energy cells: the cell $\mathfrak{C}_\nu$ (for $\nu<N/2$) includes all states within $(\xi_{\nu-1} : \xi_\nu) = (-1/\Lambda^{\nu-1} : -1/\Lambda^\nu)$. A new (Wilson) state $c_\nu^\dagger$ is a superposition of all states within an energy cell $(\xi_{\nu-1} : \xi_\nu)$ and has an (averaged) energy $(\xi_{\nu-1} + \xi_\nu)/2 = \left(-\frac{\Lambda+1}{2}\right)\frac{1}{\Lambda^\nu}$. This yields for $\Lambda = 2$ a spectrum ε_ν: $-\frac{3}{4}, -\frac{3}{8}, -\frac{3}{16}, .., -\frac{3}{2^{N/2}}, -\frac{1}{2^{N/2}}$. This spectrum is extended symmetrically to positive energies (for $\nu > N/2$). For a given N the two smallest energy cells extend from $\pm 2^{-(N/2-1)}$ to 0, and the (absolute) smallest energy levels are $\pm 2^{-N/2}$. The (absolute) smallest energies (with respect to the Fermi level) correspond to a smallest wave number Δk which is equal to $\Delta\varepsilon$ because Wilson uses the dispersion relation $\varepsilon = (k-1)$. Therefore one has $\Delta k = |k - k_F| \approx 2^{-N/2}$. Since the smallest Δk is connected with the finite size of the sample through the relation

$$R = \alpha_d \frac{\pi}{\Delta k}$$

where R is the radius of the sample and α_d is in one dimension $\alpha_1 = 1/2$ and in three dimensions $\alpha_3 = 1$. Therefore one can simulate a sample of finite size by a small number N of Wilson states. It is well known from Wilson's NRG theory that the Kondo effect occurs only for a sufficiently large N, i.e. a sufficiently large sample where the sample size is larger than the Kondo length $R_K = \hbar v_F/\varepsilon_K$.

In Fig.11 the scalar products $\left\langle a_{+,i}^\dagger \Phi_0 | a_{-,i}^\dagger \Phi_0 \right\rangle$ are plotted as a function of $\log|E_{i,+}|$ for different N or sample size. The curves for $N = 20$ (open circles) and $N = 30$ ($\triangle$) don't come close to the value of one at the smallest value of $E_{i,+}$. For $N = 40$ ($\triangledown$) the curve just

reaches the value of one and for $N = 50$ (stars) the curve assumes the value one over two decades of energy.

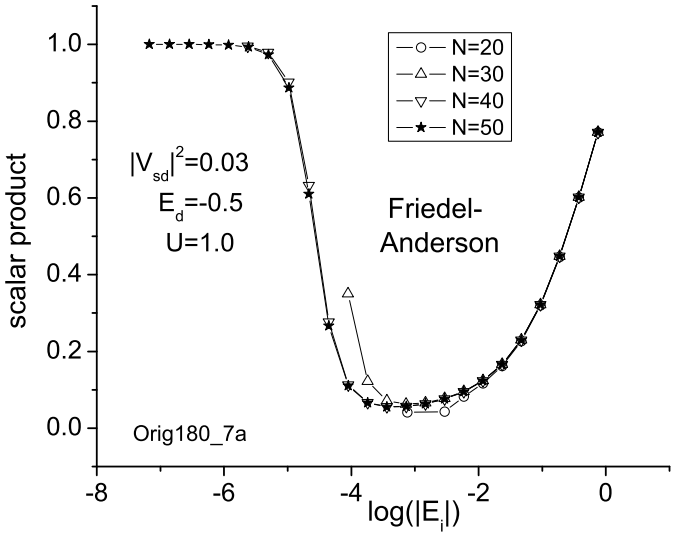

Fig.11: The scalar product $\left\langle a^\dagger_{+,i}\Phi_0|a^\dagger_{-,i}\Phi_0\right\rangle$ as a function of $\log|E_{i,+}|$ for the different number N of Wilson states for a Friedel-Anderson impurity. The parameters are $|V_{sd}|^2 = 0.03$, $E_d = -0.5$ and $U = 1.0$. Only the curves for $N = 40$ and 50 reach the value close to one.

In Fig.12 the value of the (logarithm of the) singlet-triplet excitation energy E_{st} and the corresponding Kondo energy from the susceptibility ($E_\chi = 1/4\chi$) are plotted versus the number N of Wilson states. The Kondo energy is of the order of $10^{-5} \approx 2^{-16.5}$. This corresponds to an $N_{cr} \approx 33$. And indeed one recognizes that the energies E_{st} and E_χ increase for $N < 33 \approx N_{cr}$. This value corresponds to a sample size of $R \approx 2^{16.5} \approx 10^5$.For smaller samples ($N < N_{cr}$) the two expressions for the Kondo energy loose their meaning. They don't indicate by themselves that the Kondo effect has disappeared. On the other hand the spin-up and down states close to the Fermi energy have lost their alignment (see Fig.11), showing that the Kondo effect is destroyed.

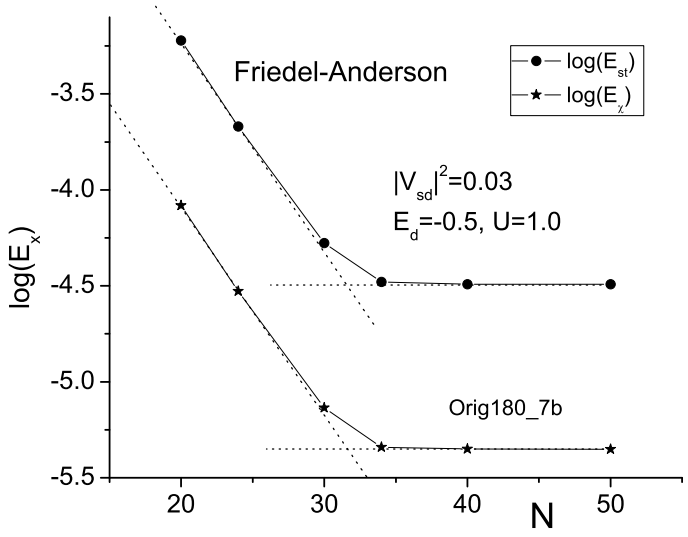

Fig.12: The (logarithm of the) singlet-triplet excitation energy E_{st} and the susceptibility energy $E_\chi = 1/4\chi$ are plotted versus the number N of Wilson states. For N larger than a a critical number $N_{cr} \approx 33$ these energies are constant but below N_{cr} both energy values increase.

References

[1] P. W. Anderson, Phys. Rev. Lett. 18, 1049 (1967) , The orthogonality catastrophe

[2] D. R. Hamann, Phys. Rev. Lett. 26, 1030 (1971) , Orthogonality Catastrophe in Metals

[3] K. Yamada and K. Yosida, Prog. Theor. Phys. 59, 1061 (1979) , Orthogonality Catastrophe Due to Local Electron Interaction

[4] K. Yamada and K. Yosida, Prog. Theor. Phys. 62, 363 (1979) , Orthogonality Catastrophe for a System of Interacting Electrons. II

[5] G. Bergmann, Phys. Rev. B 74, 144420 (2006) , Compact Approximate Solution to the Friedel-Anderson Impuriy Problem

[6] G. Bergmann, Phys. Rev. B 73, 092418 (2006) , A Critical Analysis of the Mean-Field Approximation for the Calculation of the Magnetic Moment in the Friedel-Anderson Impurity Model

[7] G. Bergmann and L. Zhang, Phys. Rev. B 76, 064401 (2007) , A Compact Approximate Solution to the Kondo Problem

[8] G. Bergmann,arXiv:0908.3887 (2009) , A Compact Treatment of the Friedel-Anderson and the Kondo Impurity Using the FAIR Method

[9] H. R. Krishna-murthy, J. W. Wilkins, and K. G. Wilson, Phys. Rev. B 21, 1003 (1980) , Renormalization-group approach to the Anderson model of dilute magnetic alloys. I. Static properties for the symmetric case

[10] K. G. Wilson, Rev. Mod. Phys. 47, 773 (1975), The renormalization group: Critical phenomena and the Kondo problem

[11] G. Bergmann,unpub (2009) , Oscillations of the magnetic polarization in a Kondo impurity at finite magnetic fields

[12] G. Bergmann, Phys. Rev. Lett. 67, 2545 (1991), Critical size of small particles for the development of resonances